Supplementary information

Part 1 Materials and Methods

Sample collection and genome sequencing

A male plateau pika (*Ochotona curzoniae*) and a female plateau zokor (*Myospalax baileyi*) were captured from Riyue Mountain (2800 m a.s.l.), Qinghai, China. Muscle tissues from both species were obtained and frozen in liquid nitrogen. High-quality genomic DNA was extracted using Gentra Puregene Tissue Kit (QIAGEN) according to the standard protocol. Sequencing libraries with different insert sizes ranging from 180 bp to 10 kb were constructed for both species and sequenced on a HiSeq2000 platform according to the manufacture's recommendation. A total of 557.9 and 460.9 Gb raw data were generated for the plateau zokor and plateau pika, respectively (**Supplementary information, Table S1**). To obtain high-quality clean data, we proposed five criteria to filter raw reads: (1) reads with > 3% of '*N*'; (2) reads with > 20% bases with the Phred score < 7; (3) reads with > 10 bp of the adapter sequence (≤ 2 bp mismatches); (4) reads with > 10 bp overlap between the two paired ends; and (5) reads from PCR duplicates. Raw reads that meet one of these criteria were discarded. In addition to Illumina libraries, three MiSeq libraries with 500 bp insert size were constructed and sequenced for the plateau zokor. A total of 29.0 Gb raw data was obtained. To acquire high-quality reads, we first removed the 3' end base one-by-one until the average quality reached ≥ 20, and then discarded a pair of reads if each of the reads contained > 20% of bases with Phred quality < 20. The remaining reads were used only for gap-closure during the genome assembly of plateau zokor. Statistics of raw data and filtered reads from all libraries were shown in

Supplementary information, Table S1.

Genome assembly

The genome sizes of the plateau pika and plateau zokor were estimated using the *K*-mer approach[1]. *K*-mer frequencies were assumed to follow a Poisson distribution in the sequenced reads and, thus, the genome size (*G*) was estimated by $G = K\_num/K\_depth$, where *K_num* indicated the total number of *K*-mers and *K_depth* was the sequencing depth of *K*-mer. Our HiSeq 2000 clean reads from libraries with insert sizes ≤ 500 bp were used for estimating genome sizes of 2.47 G for the plateau pika and 3.17 G for the plateau zokor (**Supplementary information, Table S2**). Genomes of the plateau zokor and the plateau pika were *de novo* assembled using SOAPdenovo based on the *de Bruijn* graph algorithm[2]. Briefly, we used 35- and 47-mers to construct the *de Bruijn* graphs and used Illumina clean reads with < 1000 bp to yield contig graphs. Contigs were merged into scaffolds based on the paired-end information systematically from small to large insert size libraries. Intra-scaffold gaps were filled by the local assembly using the paired-end reads of HiSeq2000, in which one end read was uniquely mapped to the contigs, while the other was located the gap region. For the plateau zokor, MiSeq reads were also used for gap closure. Finally, the N50 of contigs was 26.5 Kb for the plateau pika and 35.0 Kb for the plateau zokor; and the N50 values of scaffolds were 5.77 Mb for the pika and 4.35 Mb for the zokor (**Supplementary information, Table S3**).

Transposable element annotation

Tandem repeats were searched across the genome using Tandem Repeats Finder[3] with default parameters. Transposable elements (TEs) were identified using RepeatMask[4] against Repbase (20140131)[5] with default options, followed by *RepeatProteinMask* with the cutoff of 1.0E-05, which identified TEs by aligning the genome sequence to a self-taken curated TE protein database. For a better comparison with other mammals, we used the same pipeline and parameters to re-run the repeat annotation of human and mouse genomes. The TE content accounted for 28.73%, 31.34%, 42.31% and 37.45% in plateau pika, plateau zokor, human and mouse genome, respectively (**Supplementary information, Table S4**). TE content of the

plateau pika and plateau zokor were smaller than those of human and mouse, but similar to the naked mole rat[6].

Genome quality assessment

Three different methods were used to assess the quality of genome assemblies. First, clean reads from the small libraries of HiSeq2000 were aligned onto the assembled genome using BWA[7] with default parameters. About 99.16% and 98.93% of reads mapped to the assembled genomes and the corresponding coverage reached 98.88% and 99.66% for the plateau pika and the plateau zokor, respectively. Most of the assembled sequences (97.21% and 98.87%) were covered by at least 20 reads for the plateau pika and the plateau zokor. Second, transcripts *de novo* assembled from RNA-seq data of six tissues using Trinity[8] were aligned to the scaffolds using BLAT[9]. Using a cutoff of 90% identity, 93.01% and 98.50% of the transcripts were mapped to the scaffolds for the plateau pika and the plateau zokor, respectively. Third, the CEGMA (core eukaryotic gene mapping analysis) method[10] was used to identify the ultra-conserved core genes in each of the two genomes. Analyses found 235 (94.76%) and 246 (99.19%) out of 248 ultra-conserved core eukaryotic genes in the assembled genomes of the plateau pika and the plateau zokor, respectively (**Supplementary information, Table S5**). These results implied that we obtained high quality assembled genomes.

Annotation of protein-coding genes

The Broad Institute Eukaryotic Annotation Pipeline[11] was used to predict protein-coding genes in each of the genomes by integrating gene annotations from different prediction approaches.

Gene prediction based on sequence homology

For the homology-based prediction, we first used TblastN[12] to align human and mouse proteins against the two assembled genomes with the cutoff of E-value < 1E-5. Then, genBlastA[13] was used to cluster all the high-scoring segment pairs into gene-like structures. GeneWise (v2.4.1)[14] was used to search for accurate spliced sites of these gene-like structures by inputting the aligned sequences (extending 500 bp at both ends) and the query proteins.

Gene prediction based on transcriptome

Transcriptomes from brain, heart, liver, lung, spleen, and kidney of the plateau pika and plateau zokor were generated to aid gene prediction. The tissues were isolated from both species and preserved in Sample Protector for RNA (TaKaRa). Total RNA was extracted using the RNeasy Plus Universal kit (QIAGEN). The quality and integrity of RNA extracts were examined using the Agilent 2100 Bioanalyzer, and their RNA integrity number (RIN) values ranged from 7.5 to 9.0. Approximately 5 μg of the total RNA from each tissue was used to construct the cDNA library according to the standard protocol. The insert size of libraries was determined by the Agilent 2100 Bioanalyzer. Libraries were sequenced using the Illumina HiSeq 2000 platform with 100 bp paired-end following the manufacturer's instructions. After filtering out low-quality reads, all remaining clean reads of both species were mapped to their assembled genomes using TopHat[15] and then fed to Cufflinks[16] for transcript assembly. Transcriptome reads were used to define the gene structures (e.g. exon boundary, UTR) and the corresponding mRNA sequences were extracted from the matched genomic sequences. For the Trinity genome-guided assembly[8], high-quality transcriptome reads were mapped to the assembled genomes of both species using GSNAP package[17]. Transcriptome reads were grouped and partitioned by locus. Each locus was *de novo* assembled by Trinity. The assembled genomes were used as a guide for grouping transcriptome reads into clusters and the final transcripts were assembled based on transcriptome reads. For *de novo* assembling transcriptomes, six transcriptome reads from the same species were merged and then *de novo* assembled using Trinity package[8] with default parameters. Finally, PASA[18] (Program to Assemble Spliced Alignments) was applied to integrate the three assembled transcriptomes (TopHat/Cufflinks transcriptome, Trinity genome-guided transcriptome and Trinity *de novo* transcriptome) to obtain a consensus gene set based on overlapping transcript alignment.

De novo gene prediction

Transcripts were mapped to the assembled genomes of both species using BLAT with default parameters[9]. For each transcript, the matched genomic region with the

highest-scoring spliced alignment was selected to identify the exon boundaries followed by gene structure prediction using AUGUSTUS[19].

For homology, RNA-seq and *de novo* gene predictions were integrated using EVM (Evidence Modeler)[11] with default parameters to obtain a comprehensive and non-redundant reference gene set. The set was then subjected to PASA for further updating of EVM consensus predictions, adding UTR annotations and models for identifying alternatively spliced isoforms.

To obtain a high-quality protein-coding gene set, we retrieved 1) genes which encode ≥ 50 amino acids and could be mapped to NCBI non-redundant protein (nr) database with cutoff E < 1E-5 and (alignment length)/(query length) ≥ 0.7; 2) for single-exon genes, (alignment length)/(subject length) ≥ 0.7 was further required; and 3) genes absent in NR database but with complete predicted ORFs and with full length evidenced by RNA-seq derived transcripts. Finally, we obtained a total of 20,204 and 21,000 protein-coding genes for the plateau pika and the plateau zokor, respectively. These numbers were comparable with those from the five well-annotated mammal genomes used in this study (**Supplementary information, Table S6**).

Identification of one-to-one orthologous protein-coding genes

One-to-one orthologous protein-coding genes among human, marmoset, mouse, rabbit, dog, cow, sheep, microbat and elephant were downloaded from OrthoMaM database[20]. The genomic data of the Tibetan antelope[21] and the yak[22] gene sets were downloaded from the GenBank database and the Yak Genome Database 20 (me.lzu.edu.cn/yak/). Using the one-to-one orthologous protein-coding genes in human, dog, cow and mouse as queries to blast the protein-coding genes, we first obtained 11,836, 11,372, 10,454 and 11,383 single-copy genes in yak, antelope, plateau pika, and plateau zokor genomes, respectively. We then used Inparanoid (v4.1)[23] to obtain a total of 6,643 one-to-one orthologous protein-coding genes across these 13 mammal species.

Detection of genome-wide molecular convergence/parallel changes in protein-coding genes

PRANK[24] was used to align the coding sequences of 6,643 one-to-one

orthologous genes with the codon model. PAML[25] was used to infer ancestral sequences of each internal node based on the species tree (**Fig. 1a**). Only the inferred codons with probability ≥ 0.95 were retrieved for detecting convergent/parallel changes. We used in-house Perl scripts to identify potential convergent/parallel amino acids among the plateau species for each of the one-to-one orthologous genes. A convergent amino acid change referred to changes from a different ancestral amino acid to the same descendant amino acid in independent evolutionary lineages, whereas a parallel amino acid change referred to a change from the same ancestral amino acid to the same descendant amino acid[26]. To minimize false positives after identifying parallel sites, we first downloaded all other mammalian genomes with high quality (Sanger sequencing coverage ≥ 6x) from Ensembl, including chimpanzee, orangutan, gorilla, macaque, rat, pig, horse and Guinea pig, to test whether the identified parallel sites were reliable. If a parallel amino acid was also found to occur in more than two of these mammals, we discarded the site. Second, detecting convergence at conservative sites can drastically reduce random convergence at rapidly evolving sites as well as falsely inferred convergence caused by the mis-inference of the ancestral character[27]. Thus, we removed parallel amino acid changes located in the poorly aligned fragments (10 amino acids flanking the convergent site). Poorly aligned fragments referred to those with one of the following criteria: 1) mean sequence similarity < 0.7; 2) lowest similarity < 0.35 between any two species; and 3) > 5 indels present in more than two species. Third, a statistical test was used to determine whether the observed convergent/parallel sites occur by chance or by selection by comparing with a null hypothesis derived from neutral evolution[28]. In principle, convergences are first inferred based on the evolutionarily neutral substitution models JTT-f_{gene} and JTT-f_{site} for two or multiple independent branches. Then, one can test whether the observed molecular convergences are significantly more than those neutrally expected according to Poisson distribution[28, 29]. The *P* values were adjusted by false discovery rate correction and only convergent/parallel genes with q value < 0.05 were retained. The same searching strategy was also used to identify the molecular convergent/parallel evolution in protein-coding genes among

the lowland relatives of the QTP species.

Phenotype enrichment analyses for the parallel genes

Phenotype terms associated with each parallel gene were retrieved from MGI 6.13 database (www.informatics.jax.org). The total number of MP (Mammalian Phenotype) items and the number of MP items involving in heart development were counted for the parallel genes among the QTP mammalian species and among their lowland relatives, respectively (**Supplementary Information, Table S8, S9**). The ratio of the number of MP items related to heart development to the total number of MP items was compared between the QTP mammalian species and their lowland relatives.

Enzymatic activity assay of RETSAT

Intact coding sequences of mouse wild-type RETAST (247Q) and mutant (247R) were synthesized and cloned into pCDH-eGFP-3xFlag lenti-viral vector. HEK-293T cells stably expressing *RETSAT*$^{Q/Q}$ or *RETAST*$^{R/R}$ were incubated with retinoid substrates (Sigma. R7632) for 24 hrs in 6-well plates, and indicated cell lysates were then harvested and analyzed by HPLC following the previously published protocol [30]. Briefly, the cells in each well were suspended in 500 µl PBS and then acetonitrile/butanol solution (350 µl, 1:1 *vol*/*vol*) was added and vortexed for 45 seconds. Saturated K_2HPO_4 was added and vortexed for 15 seconds. After centrifugation (10 minutes; 20,000 g) at 22 °C, the upper organic phase was separated and transferred into a new tube for additional centrifugation (5 minutes; 20,000 g) at 22 °C to remove nonorganic components. The supernatants were used for HPLC analysis. Each sample was added into an analytic 5-µm reverse-phase C18 column (Waters) at a flow rate of 1.0 ml/min in a Waters Empower system. HPLC program was set following the standard protocol[30], and the samples were eluted from the C18 column by water/acetonitrile elution system containing 0.1% trifluoroacetic acid, and a 52.5-minute linear gradient of solvent B from 40% to 100% was used, which were monitored at both 290 nm and 325 nm.

Generation of transgenic engineering mice carrying arginine at position 247 of RETSAT

To generate transgenic engineering mice with the parallel amino acid arginine at position 247 in RETSAT (*RETSAT*$^{R/R}$) using the CRISPR/Cas9 method, we selected the sgRNA target sequence (CCTGCAGCAGCTTGGGGCTTCCC) of murine *RETSAT* to direct Cas9 cleavage. Cas9 mRNA and sgRNA were purified using RNA Clean & Concentrator-25 (ZYMO Research) and dissolved in RNase-free water. RNA concentrations were measured using a NanoDrop ND1000. Finally, 2μl of each of sgRNA and Cas9 mRNA were mixed with an equal volume of formamide. We ran 800 ng of sgRNA and Cas9 mRNA on a DNA agarose gel to evaluate RNA quality. We designed and synthesized four 120 bp single-stranded donors respectively containing four synonymous codons of *R* (CGG, CGC, CGU, and CGA) to create the transgenic mice (Q247R) simultaneously. . The mixture of sgRNA, Cas9 mRNA and oligo DNA in RNAase-free water was injected into the cytoplasm of C57BL/6 inbred zygotes. After injection, surviving zygotes were transferred immediately into oviducts of ICR albino pseudopregnant females. These female mice were maintained under cycles of 12-hour light and 12-hour dark. The *RETSAT* genotypes of the generated mouse strains were confirmed by sequencing (Forward primer: CAGTAACTAGGCTCCAGCAC; Reverse primer: GCCTGGGGCTATTCTAGCCT). Finally, the transgenic engineering mice (Q247R) were obtained by mutating AG into GC. Mice with different genotypes were generated by crossing with C57BL/6. All animal operations were approved by the Animal Care and Use Committee of Kunming Institute of Zoology, Chinese Academy of Sciences.

Measurement of the heart mass to body mass ratio

The body mass of mice was measured in deep anesthesia with pentobarbital sodium (112.5 mg/kg). The heart was dissected and washed with ice-cold phosphate buffer (PBS) to remove the blood and other residual tissues. The remained PBS in the heart was drained with filter paper. Then, the heart mass was measured and the ratio of heart mass to body mass was calculated[31].

Echocardiographic analysis

Transthoracic closed-chest echocardiography was performed using a mechanical transducer centered on 40 MHz (Vevo3100, Visualsonics, Canada). Briefly, 8- to 10-

week-old wild-type *(RETSAT*$^{Q/Q}$) or transgenic (*RETSAT*$^{R/R}$) mice were light anesthetized with 0.3L/min mix gas (1.5% isoflurane and 98.5% oxygen). Then, hair was shaved and smeared with coupling agents over the measurement area. The mice were then placed in a supine position on a heating pad which was maintained at 38.5℃. After the heart rate dropping to 450~500 beats/min, two-dimensional images were started to be obtained. All analyses were done with the Cardiac Package (VisualSonics). Pulmonary artery diameter (PAD) was measured from the parasternal long-axis views just distal to the valve leaflets with the B-mode[32]. Pulmonary strove volume (SV) was calculated as the product of VTI and the vessel area ($A = 1/4 \times \pi \times PAD^2$)[32]. Pulmonary cardiac output was obtained as the product of SV and the heart rate [32]. Pulmonary flows, including the parameters of velocity-time integral (VTI), pulmonary artery acceleration time (PAT), and pulmonary ejection time (PET), were measured with the pulsed-wave Doppler model from the same position where the PAD obtained. The final VTI, PAT, and PET were calculated as the mean of three random cardiac cycles in a 300ms-interval while avoiding the respiratory peaks. Right ventricular systolic pressure (RVSP) was calculated as the function of the PAT value (**Supplementary information, Fig. S4b**) or the PAT/PET value (**Fig. 1h**) following the previous study[33].

Histology

Hearts were collected and weighted without fat tissues for the *RETSAT*$^{Q/Q}$ and *RETSAT*$^{R/R}$ strains. For histology, hearts were fixed in 4% paraformaldehyde overnight at room temperature and dehydrated as the following steps: 70% ethanol, 30 minutes; 80% ethanol, 30 minutes; 90% ethanol, 30 minutes; 90% ethanol, 30 minutes; 100% ethanol, 15 minutes; 100% ethanol, 15 minutes. Next, samples were moved into xylene for 30 minutes twice and embedded with paraffin (Leica). Paraffin sections (4 μm), spanning the entire heart, were cut using a rotary microtome. The sections were de-waxed in xylene twice and rehydrated by a series of 100%, 95%, 85%, 75% ethanol, and ddH_2O. Hematoxylin-eosin staining was performed following the protocols previously described[34].

Survival experiment of transgenic and wild-type mice in acute hypoxia

The transgenic mice (*RETSAT*$^{R/R}$) and their wild-type littermates (*RETSAT*$^{Q/Q}$) were placed in a sealed box (BioSpherix, USA), and the inlet of the box was connected to gas tanks balanced by N_2 to create different O_2 concentration. Indicated mice were exposed to reduced inspired O_2 levels from 21 to 4% O_2. In detail, mice were exposed to 15% O_2 for 10 minutes, and 10% O_2 for additional 10 minutes, then finally to 4% O_2 until death. The time to mortality was measured at 4% O_2[35].

Pimonidazole immunohistochemistry

The pimonidazole immunohistochemistry was performed according to the procedures previously described[35]. Awake mice received an infusion of the hypoxic marker Hypoxyprobe-1 [pimonidazole, 60 mg/kg (Hypoxyprobe Incorporation)] and 5 mg/kg Hoechst 33342 (Invitrogen) diluted in PBS with a total volume of 100 μl when they were exposed to 10% O_2 level. Then, the mice received a second infusion of pimonidazole and Hoechst 33342 when they were exposed to 5% O_2. Finally, indicated mortal mice exposed to 4% O_2 were euthanized and their vital organs (brain, heart, kidney, intestine, and liver) were collected. These tissues were fixed by immersion in 4% paraformaldehyde for 24 hours at 4℃. The tissues were sectioned into 100 μm pieces with the Vibratome machine (LEICA, VT1000S). Pimonidazole staining was performed according to the manufacture protocol (included in the HypoxyprobeTM-1 Green Kit: HP-100mg). Fluorescence signals were captured using a Nikon ECLIPSE Ti equipped with a high-resolution digital camera. Positive areas of pimonidazole staining were quantified by Image J software. Mouse embryonic fibroblasts (MEFs) were isolated from E13.5 embryos from *RETSAT*$^{Q/Q}$ or *RETSAT*$^{R/R}$ mice. Indicated 5×10^4 MEFs were seeded in the 8-well plates incubated with 20 μM pimonidazole and treated by 1% O_2 for additional 2 hours. Then, indicated cells were fixed and stained following the above detailed procedure. The ratio of pimonidazole positive staining in each region to the total cellular area of the image was calculated.

Selection test of the parallel substitution in mammals

The RETSAT protein sequences of a total of 137 mammalian species (Supplementary table S11) were downloaded from the Genbank database

(www.ncbi.nlm.nih.gov/genbank/) and the Ruminant Genome Project (http://animal.nwsuaf.edu.cn/code/index.php/RGD). After being aligned using PRANK, we estimated the expected number of parallel substitutions under the neutral evolutionary model[36] along the lineages with Q247R according to the phylogeny of mammals in this study[37, 38]. We tested whether the observed molecular parallel is significantly more than those neutrally expected by following Poison distribution.

REFERENCES

1 Li, R et al. *Nature*. **463**:311-317 (2010).
2 Luo, R et al. *Gigascience*. **1**:18 (2012).
3 Benson, G. *Nucleic Acids Res*. **27**:573-580 (1999).
4 Tarailo-Graovac, M et al. *Curr Prot Bioinform*. **25**:4.10. 11-14.10. 14 (2009).
5 Jurka, J et al. *Cytogenet Genome Res*. **110**:462-467 (2005).
6 Kim, EB et al. *Nature*. **479**:223-227 (2011).
7 Li, H et al. *Bioinformatics*. **25**:1754-1760 (2009).
8 Grabherr, MG et al. *Nat Biotechnol*. **29**:644-U130 (2011).
9 Kent, WJ. *Genome Res*. **12**:656-664 (2002).
10 Parra, G et al. *Bioinformatics*. **23**:1061-1067 (2007).
11 Haas, BJ et al. *Genome Biol*. **9**:R7 (2008).
12 Altschul, SF et al. *J Mol Biol*. **215**:403-410 (1990).
13 She, R et al. *Genome Res*. **19**:143-149 (2009).
14 Birney, E et al. *Genome Res*. **14**:988-995 (2004).
15 Trapnell, C et al. *Bioinformatics*. **25**:1105-1111 (2009).
16 Mortazavi, A et al. *Nat Methods*. **5**:621-628 (2008).
17 Wu, TD et al. *Bioinformatics*. **26**:873-881 (2010).
18 Haas, BJ et al. *Nucleic Acids Res*. **31**:5654-5666 (2003).
19 Stanke, M et al. *Bioinformatics*. **19 Suppl 2**:ii215-225 (2003).
20 Douzery, EJP et al. *Mol Biol Evol*. **31**:1923-1928 (2014).
21 Ge, RL et al. *Nat Commun*. **4**:1858 (2013).
22 Qiu, Q et al. *Nat Genet*. **44**:946-949 (2012).
23 Remm, M et al. *J Mol Biol*. **314**:1041-1052 (2001).
24 Loytynoja, A et al. *Proc Natl Acad Sci USA*. **102**:10557-10562 (2005).
25 Yang, ZH. *Mol Biol Evol*. **24**:1586-1591 (2007).
26 Zhang, J et al. *Mol Biol Evol*. **14**:527-536 (1997).
27 Xu, S et al. *Mol Biol Evol*. **34**:1008-1015 (2017).
28 Zou, Z et al. *Mol Biol Evol*. **32**:2085-2096 (2015).
29 Zhang, J et al. *Mol Biol Evol*. **14**:527-536 (1997).
30 Schupp, M et al. *Proc Natl Acad Sci USA*. **106**:1105-1110 (2009).
31 Qi, X et al. *Sheng li xue bao:[Acta physiologica Sinica]*. **60**:348-354 (2008).

32 Platt, MJ et al. *J Am Soc Echocardiogr*. **30**:612-+ (2017).
33 Thibault, HB et al. *Circ Cardiovasc Imaging*. **3**:157-163 (2010).
34 He, LJ et al. *Plos One*. **9**:e109493 (2014).
35 Stobdan, T et al. *Proc Natl Acad Sci USA*. **112**:10425-10430 (2015).
36 Zou, ZT et al. *Mol Biol Evol*. **32**:2085-2096 (2015).
37 Scornavacca, C et al. *Mol Biol Evol*. **36**:861-862 (2019).
38 Chen, L et al. *Science*. **364** (2019).

Part 2 Supplementary Figures

Supplementary information, Fig. S1. Western blotting result of the RETSAT protein. No significant difference in the protein expression level between the wild-type *RETSAT*$^{Q/Q}$ and mutant *RETSAT*$^{R/R}$ in HEK293T cells. The *P* value is from the two-tailed Student's *t*-test.

Supplementary information, Fig. S2. Genotyping for the wild-type (WT; *RETAST*$^{Q/Q}$) and transgenic (TG; *RETSAT*$^{R/R}$) mice.

Supplementary information, Fig. S3. Comparison of heart mass and body mass between the wild-type (WT; *RETSAT*$^{Q/Q}$) and transgenic (TG; *RETSAT*$^{R/R}$) mice. a. Hematoxylin and eosin-stained four-chamber views of hearts for the TG and WT mice. IVS, interventricular septum; LV: left ventricle; RV: right ventricle; LA: left atrium; RA: right atrium. b. Heart mass is significantly larger for the TG mice than for the WT mice. c. No significant different in body mass between the TG and the WT mice. Boxes indicate the first, the median, and the third quartile. Whiskers denote upper and lower bounds. The *P* values are from the two-tailed Student's *t*-tests.

Supplementary information, Fig. S4. Echocardiography analyses between the TG and WT mice. a. Pulmonary cardiac output is significantly higher for the TG mice than for the WT mice. b. Right ventricular systolic pressure (RVSP) is significantly lower for the TG mice than for the WT mice. The value of RVSP shows a negative correlation with PAT value according to the previous study (see Methods). The formula is as follows: RVSP = -1.5×PAT+63.7. Boxes indicate the first, the median, and the third quartile. Whiskers denote upper and lower bounds. The P values are from the two-tailed Student's *t*-tests.

Supplementary information, Fig. S5. Higher oxygen saturation levels in liver blood for the TG mice than for the WT mice. The P value is from the two-tailed Student's *t*-test.

Supplementary information, Fig. S6. The TG mice live significantly longer in the acute hypoxic condition (4% O2) compared with the WT mice for both females and males.

Supplementary information, Fig. S7. Enhanced hypoxia tolerance of the TG mice. Representative images of the hypoxic indicator pimonidazole dye for mouse embryonic fibroblast cells (a), brain (b), heart (c), liver (d), kidney (e) and spleen (f) from the WT and TG mice. Areas with pimonidazole dye shown in green and blue indicate DAPI and Hoechst staining. The statistical analysis results are shown in Fig. 1j.

Supplementary information, Figure S1

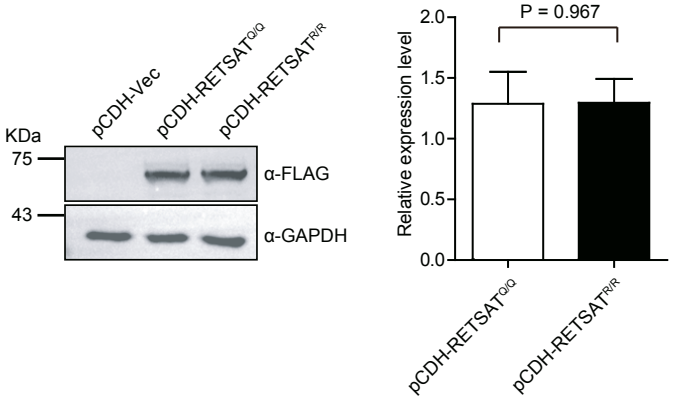

Supplementary information, Figure S2

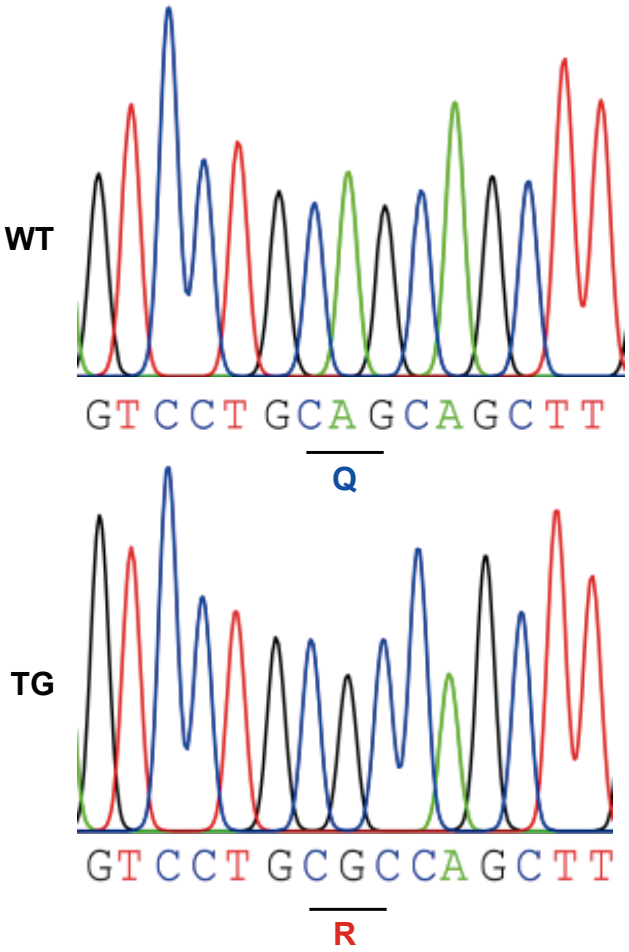

Supplementary information, Figure S3

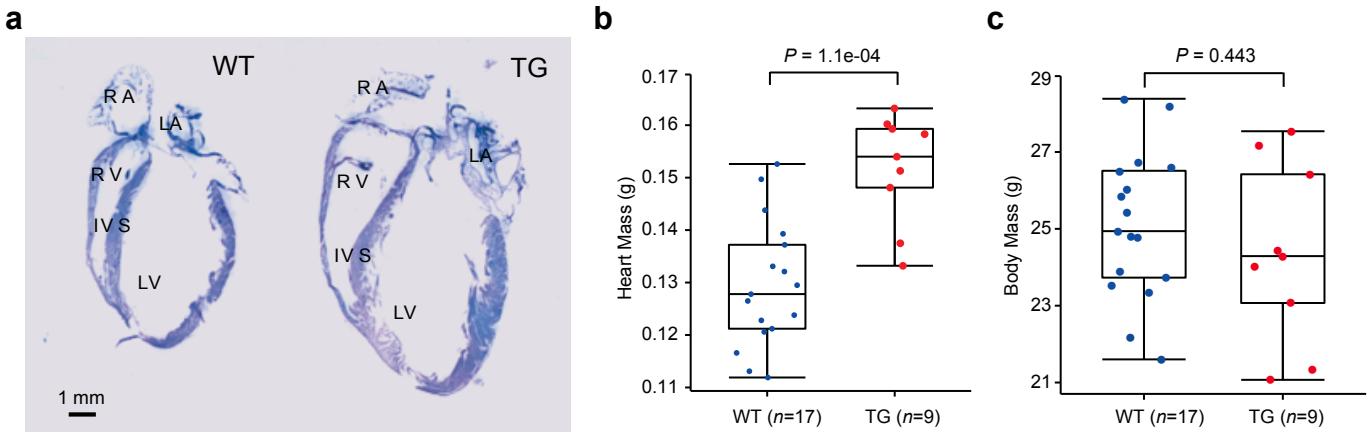

Supplementary information, Figure S4

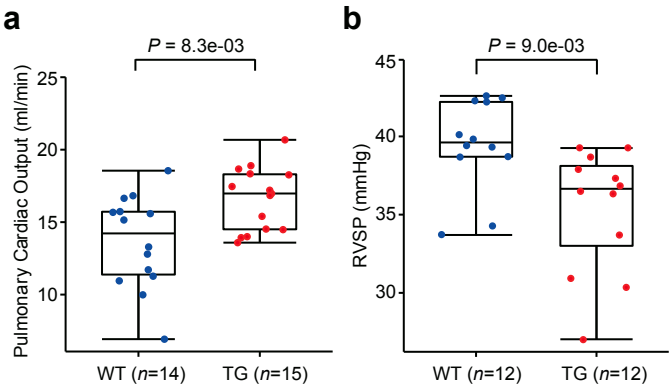

Supplementary information, Figure S5

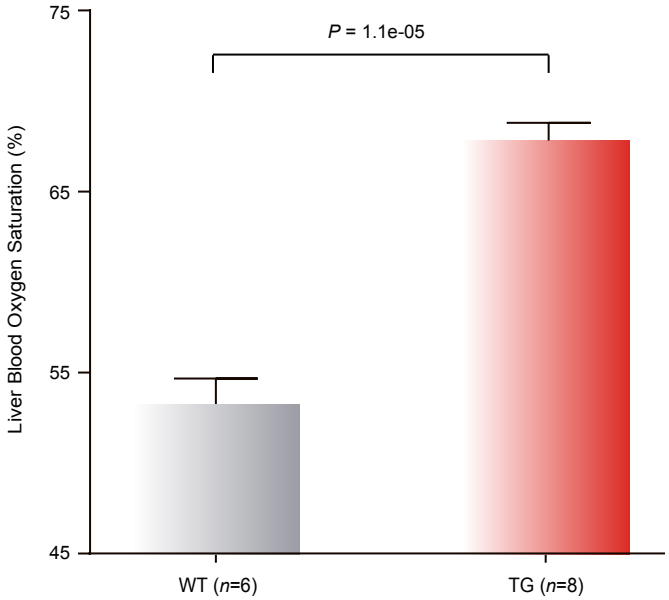

Supplementary information, Figure S6

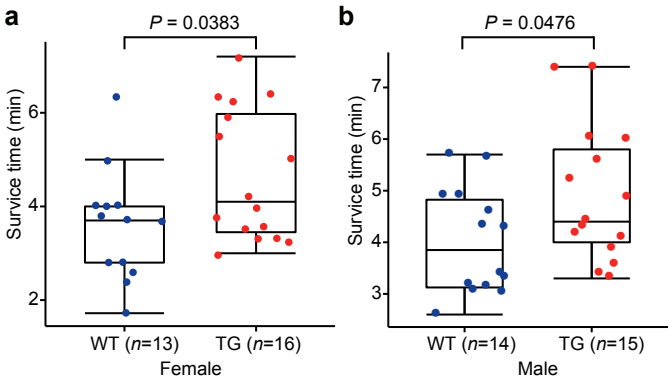

Supplementary information, Figure S7

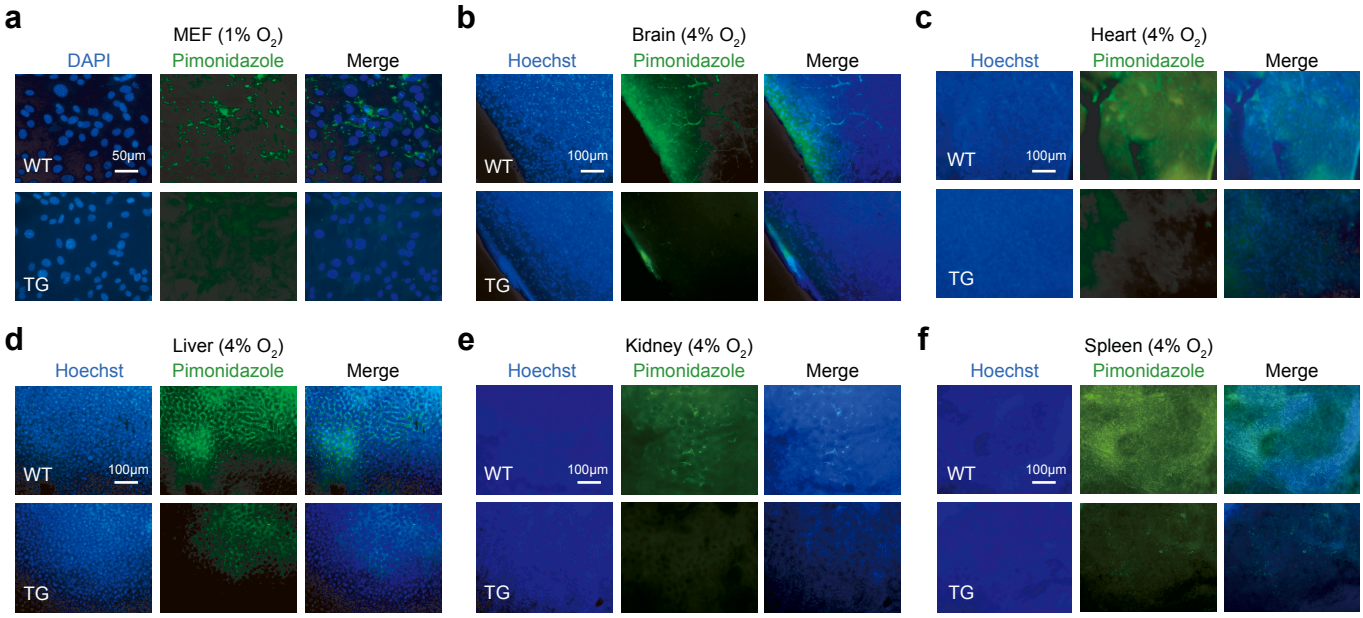

Table S1: Summary of genome sequencing of *Myospalax baileyi* and *Ochotona curzoniae*

Specie	Platform	Insert size (bp)	# of Library	Raw data (Gb)	Clean data (Gb)	Read length (bp)	Sequence coverage (X)	Physical coverage (X)
Plateau zokor (*Myospalax baileyi*)	Hiseq	180	4	120.9	108.6	100	34.3	30.8
		300	1	43.0	41.5	100	13.1	19.6
		500	1	44.0	41.0	100	12.9	32.3
	Miseq	500	3	29.0	19.7	300	6.2	6.1
	Hiseq	800	1	42.4	33.6	100	10.6	42.4
		3,000	5	141.8	91.5	100/101	28.9	433.0
		5,000	3	45.3	25.2	100	7.9	198.7
		8,000	2	79.9	37.0	101	11.7	466.9
		10,000	2	40.6	15.7	101	5.0	247.6
	Total		22	586.9	413.8		130.5	1477.5
Plateau pika (*Ochotona curzoniae*)	Hiseq	180	4	113.8	109.9	100	44.5	40.0
		250	1	47.7	37.5	100	15.2	19.0
		500	1	42.4	33.9	100	13.7	34.3
		800	1	46.4	29.6	100	12.0	47.9
		3,000	2	85.4	45.7	101	18.5	277.8
		8,000	2	82.9	24.1	101	9.8	389.8
		10,000	2	42.2	14.6	101	5.9	295.3
	Total		13	460.9	295.2		119.6	1104.1

Table S2: Genome size estimation for two sepcies using 17-Kmer approach

Specie	K	Number	Depth	Genome size	Coverage (X)
Myospalax baileyi	17	104,581,048,004	33	3,169,122,666	41.25
Ochotona curzoniae	17	162,872,024,879	66	2,467,757,952	79.55

Table S3: Summary of the genome assemblies

Specie	Parameter	Contig		Scaffold	
		Size (bp)	Number	Size (bp)	Number
Plateau zokor (*Myospalax baileyi*)	N90	4,148	94,207	31,699	1,927
	N80	12,117	59,158	1,117,799	519
	N70	19,403	42,011	2,167,831	346
	N60	26,855	30,384	3,145,243	241
	N50	35,007	21,704	4,350,784	168
	Longest	315,032		31,113,187	
	Total size	2,661,746,966		2,719,408,481	
	Total size (>100 bp)	2,661,543,316		2,719,408,432	
	Total size (>2000 bp)	2,456,016,691		2,550,109,979	
Plateau pika (*Ochotona curzoniae*)	N90	5,642	87,362	749,832	482
	N80	10,805	60,642	1,921,288	308
	N70	15,753	44,318	2,812,341	214
	N60	20,831	32,515	4,074,676	150
	N50	26,533	23,402	5,766,044	105
	Longest	391,682		30,223,653	
	Total size	2,141,214,947		2,187,936,244	
	Total size (>100 bp)	2,141,117,758		2,187,935,958	
	Total size (>2000 bp)	2,049,963,661		2,132,229,079	

Table S4: TE comparison between *Myospalax baileyi*, *Ochotona curzoniae* and other mammalian genomes

Type	Plateau zokor		Plateau pika		Mouse		Human	
	# of base	% of genome	# of base	% of genome	# of base	% of genome	# of base	% of genome
DNA	34,337,376	1.33	30,837,380	1.47	26,747,513	0.95	110,281,298	3.42
LINE	293,164,440	11.38	177,300,361	8.50	472,723,145	16.86	556,036,765	17.24
LTR	177,025,670	6.87	59,403,599	2.84	313,909,763	11.20	282,903,970	8.77
SINE	300,684,928	11.67	332,814,331	15.57	200,359,456	7.15	406,168,793	12.59
Unclassified	2,348,905	0.09	431,769	0.02	36,164,560	1.29	9,681,707	0.30
Total	807,561,319	31.34	600,787,440	28.73	1,049,904,437	37.45	1,365,072,533	42.31

Table S5: Summary of the completeness of the assembled genomes based on 248 CEGs

Specie		# of Protein[1]	Completeness (%)[2]	Total[3]	Average[4]	Orthologs (%)[5]
Plateau zokor	**Complete[6]**	**238**	**95.97**	**352**	**1.48**	**33.61**
(*Myospalax baileyi*)	**Partial[6]**	**246**	**99.19**	**501**	**2.04**	**54.47**
Plateau pika	**Complete**	**219**	**88.31**	**314**	**1.43**	**31.51**
(*Ochotona curzoniae*)	**Partial**	**235**	**94.76**	**422**	**1.8**	**42.98**

Notes: [1] Number of protein in 248 ultra-conserved core eukaryotic genes (CEGs) presenting in genome. [2]Percentage of 248 ultra-conserved CEGs presenting in genome. [3]Total number of CEGs identified in genome. [4]Average number of orthologs per CEG. [5]Percentage of detected CEGs that have more than one orthologs. [6]Complete and partial are defined by default cutoff profile.

Table S6: Summary of annotated protein-coding genes

Species	Gene number	# of genes with single exon	Average length of transcripts (bp)	Average length of ORFs (bp)	Average number of exons per gene	Average length of exons (bp)	Average length of introns (bp)
Plateau zokor	21,000	3,405	36,219	1,544	8.48	181.12	4,097
Plateau pika	20,204	2,692	38,708	1,602	9.06	175.70	4,198
Human	20,362	2,288	56,840	1,693	9.73	173.97	5,465
Mouse	22,539	3,817	42,593	1,578	8.82	178.88	4,507
Rat	21,977	3,699	36,336	1,542	8.90	173.14	3,998
Sheep	20,921	2,053	38,147	1,559	9.62	162.13	3,947
Rabbit	19,293	2,504	43,771	1,590	9.57	166.24	4,684

Table S7: Parallel evolution genes identified among different plateau mammals

Comparisons	Number of parallel evolution genes	Ensembl ID	Symbol	Observed number of parallel substitutions	Expected number of parallel substitutions (JTT-f_{gene})[1]	Expected number of parallel substitutions (JTT-f_{site})[1]
Yak vs. Tibetan antelope vs. Plateau pika vs. Plateau zokor	1	ENSG00000042445	*RETSAT*	1(Q247R)	0.00000033***	0.00088591***
Yak vs. Tibetan antelope vs. Plateau pika	3	ENSG00000109618	*SEPSECS*	1(I60V)	0.00001241***	0.00049098***
		ENSG00000139973	*SYT16*	1(R209C)	0.00018374***	0.01458612*
		ENSG00000164535	*DAGLB*	1(T316A)	0.00040758***	0.00717473**
Yak vs. Tibetan antelope vs. Plateau zokor	1	ENSG00000165323	*FAT3*	1(M3580V)	0.00001514***	0.00506537**
Yak vs. Plateau pika vs. Plateau zokor	4	ENSG00000121742	*GJB6*	1(S138G)	0.00014142***	0.00317107**
		ENSG00000181192	*DHTKD1*	1(R246Q)	0.00033846***	0.01049341*
		ENSG00000096872	*IFT74*	1(A9T)	0.00029526***	0.03317900*
		ENSG00000154781	*CCDC174*	1(S407G)	0.00006598***	0.00461357**
Tibetan antelope vs. Plateau pika vs. Plateau zokor	7	ENSG00000178217	*SH2D4B*	1(R228G)	0.00009132***	0.03194567*
		ENSG00000066056	*TIE1*	1(I704V)	0.00002873***	0.00669863**
		ENSG00000024862	*CCDC28A*	1(D233E)	0.00004729***	0.00270291**
		ENSG00000181856	*SLC2A4*	1(A364T)	0.00003435***	0.00529026**
		ENSG00000168216	*LMBRD1*	1(P262S)	0.00030826***	0.01382105*
		ENSG00000117009	*KMO*	1(S339N)	0.00069265**	0.03576839*
		ENSG00000030582	*GRN*	1(L261I)	0.00133516**	0.02950143*

Note: [1]The expected number of parallel amino acid substitution and a statistical test were conducted followed the method developed by Zou and Zhang (2015). *, P value < 0.05; **, P value <0.01; ***, P value <0.001.

Table S8: Parallel evolution genes identified among different lowland mammals

Comparisons	Number of parallel evolution genes	Ensembl ID	Symbol	Observed number of parallel substitutions	Expected number of parallel substitutions (JTT-f_{gene})[1]	Expected number of parallel substitutions (JTT-f_{site})[1]
Cow vs. Sheep vs. Rabbit vs. Mouse	0	-	-	-	-	-
Cow vs. Sheep vs. Rabbit	1	ENSG00000096968	*JAK2*	1(I711V)	0.00000167***	0.00034160***
Cow vs. Sheep vs. Mouse	2	ENSG00000138592	*USP8*	1(I330V)	0.00000682***	0.00060759***
		ENSG00000177511	*ST8SIA3*	1(H158R)	0.00000805***	0.00036698***
Cow vs. Rabbit vs. Mouse	1	ENSG00000111897	*SERINC1*	1(I213V)	0.00001416***	0.0001133***
Sheep vs. Rabbit vs. Mouse	7	ENSG00000123610	*TNFAIP6*	1(A246T)	0.00003644***	0.01096739*
		ENSG00000164292	*RHOBTB3*	1(T429A)	0.00010756***	0.00355594**
		ENSG00000065609	*SNAP91*	1(T429A)	0.00000801***	0.00745884**
		ENSG00000145794	*MEGF10*	1(I863V)	0.00003500***	0.01713733*
		ENSG00000146576	*C7ORF26*	1(S348A)	0.00004625***	0.00304808**
		ENSG00000014123	*UFL1*	1(A567T)	0.00031683***	0.01914555*
		ENSG00000183763	*TRAIP*	1(D323N)	0.00131932**	0.01681780*

Note: [1]The expected number of parallel amino acid substitution and a statistical test were conducted followed the method developed by Zou and Zhang (2015). *, P value < 0.05; **, P value <0.01; ***, P value <0.001.

Table S9: Parallel genes among plateau mammals with known phenotypes in Mouse Genome Informatics (MGI) database

Symbol	MGI Gene ID	Gene name	MP ID	Term
IFT74	MGI:1914944	intraflagellar transport 74	MP:0000284	double outlet right ventricle
			MP:0002132	abnormal respiratory system morphology
			MP:0004133	heterotaxia
			MP:0006063	abnormal inferior vena cava morphology
			MP:0010406	common atrium
			MP:0010412	atrioventricular septal defect
			MP:0010975	abnormal lung lobe morphology
			MP:0011667	double outlet right ventricle with atrioventricular septal defect
LMBRD1	MGI:1915671	LMBR1 domain containing 1	MP:0004039	abnormal cardiac cell glucose uptake
			MP:0011100	preweaning lethality, complete penetrance
			MP:0013292	embryonic lethality prior to organogenesis
			MP:0013293	embryonic lethality prior to tooth bud stage
			MP:0030018	increased cardiac cell glucose uptake
SLC2A4	MGI:95758	solute carrier family 2 (facilitated glucose transporter), member 4	MP:0000188	abnormal circulating glucose level
			MP:0000231	hypertension
			MP:0000266	abnormal heart morphology
			MP:0000343	altered response to myocardial infarction
			MP:0001262	decreased body weight
			MP:0001544	abnormal cardiovascular system physiology
			MP:0001547	abnormal lipid level
			MP:0001559	hyperglycemia
			MP:0001625	cardiac hypertrophy
			MP:0001669	abnormal intestinal glucose absorption
			MP:0001732	postnatal growth retardation
			MP:0001853	heart inflammation
			MP:0002078	abnormal glucose homeostasis
			MP:0002079	increased circulating insulin level
			MP:0002083	premature death
			MP:0002106	abnormal muscle physiology
			MP:0002118	abnormal lipid homeostasis
			MP:0002628	hepatic steatosis
			MP:0002702	decreased circulating free fatty acid level
			MP:0002833	increased heart weight
			MP:0002837	dystrophic cardiac calcinosis
			MP:0002953	thick ventricular wall
			MP:0002841	impaired skeletal muscle contractility

Symbol	MGI Gene ID	Gene name	MP ID	Term
			MP:0003058	increased insulin secretion
			MP:0003458	decreased circulating ketone body level
			MP:0003633	abnormal nervous system physiology
			MP:0003646	muscle fatigue
			MP:0003822	decreased left ventricle systolic pressure
			MP:0004819	decreased skeletal muscle mass
			MP:0005282	decreased fatty acid level
			MP:0005291	abnormal glucose tolerance
			MP:0005293	impaired glucose tolerance
			MP:0005318	decreased triglyceride level
			MP:0005329	abnormal myocardium layer morphology
			MP:0005331	insulin resistance
			MP:0005438	abnormal glycogen homeostasis
			MP:0005439	decreased glycogen level
			MP:0005440	increased glycogen level
			MP:0005491	pancreatic islet hyperplasia
			MP:0005559	increased circulating glucose level
			MP:0005608	cardiac interstitial fibrosis
			MP:0006085	myocardial necrosis
			MP:0006086	decreased body mass index
			MP:0006094	increased fat cell size
			MP:0009283	decreased gonadal fat pad weight
			MP:0009409	abnormal skeletal muscle fiber type ratio
			MP:0010025	decreased total body fat amount
			MP:0010400	increased liver glycogen level
			MP:0030016	increased adipocyte glucose uptake
			MP:0030017	decreased adipocyte glucose uptake
			MP:0030018	increased cardiac cell glucose uptake
			MP:0030020	decreased cardiac cell glucose uptake
			MP:0030021	increased muscle cell glucose uptake
			MP:0030022	decreased muscle cell glucose uptake
TIE1	MGI:99906	tyrosine kinase with immunoglobulin-like and EGF-like	MP:0000496	abnormal small intestine morphology
			MP:0001179	thick pulmonary interalveolar septum
			MP:0001785	edema
			MP:0001786	skin edema
			MP:0001914	hemorrhage
			MP:0001879	abnormal lymphatic vessel morphology

Symbol	MGI Gene ID	Gene name	MP ID	Term
			MP:0001953	respiratory failure
			MP:0002082	postnatal lethality
			MP:0002169	no abnormal phenotype detected
			MP:0002188	small heart
			MP:0002270	abnormal pulmonary alveolus morphology
			MP:0003105	abnormal heart atrium morphology
			MP:0003227	abnormal vascular branching morphogenesis
			MP:0003288	intestinal edema
			MP:0003542	abnormal vascular endothelial cell development
			MP:0003659	abnormal lymph circulation
			MP:0003828	pulmonary edema
			MP:0003974	abnormal endocardium morphology
			MP:0004106	lymphatic vessel hyperplasia
			MP:0004938	dilated vasculature
			MP:0005325	abnormal renal glomerulus morphology
			MP:0006055	abnormal vascular endothelial cell morphology
			MP:0008778	abnormal lymphangiogenesis
			MP:0011087	neonatal lethality, complete penetrance
			MP:0011089	perinatal lethality, complete penetrance
			MP:0011099	lethality throughout fetal growth and development, complete penetrance
			MP:0011101	prenatal lethality, incomplete penetrance
			MP:0011108	embryonic lethality during organogenesis, incomplete penetrance
CCDC174	MGI:2444652	coiled-coil domain containing 174	MP:0006205	embryonic lethality between implantation and somite formation
DAGLB	MGI:2442032	diacylglycerol lipase, beta	MP:0001547	abnormal lipid level
			MP:0003632	abnormal nervous system morphology
			MP:0009967	abnormal neuron proliferation
FAT3	MGI:2444314	FAT atypical cadherin 3	MP:0001325	abnormal retina morphology
			MP:0005240	abnormal amacrine cell morphology
			MP:0006069	abnormal retinal neuronal layer morphology
			MP:0006074	abnormal retinal rod bipolar cell morphology
			MP:0008508	thick retinal ganglion layer
GJB6	MGI:107588	gap junction protein, beta 6	MP:0000043	organ of Corti degeneration
			MP:0000048	abnormal stria vascularis morphology
			MP:0000647	abnormal sebaceous gland morphology
			MP:0000652	enlarged sebaceous gland
			MP:0001242	hyperkeratosis
			MP:0001216	abnormal epidermal layer morphology

Symbol	MGI Gene ID	Gene name	MP ID	Term
			MP:0001363	increased anxiety-related response
			MP:0001967	deafness
			MP:0002757	decreased vertical activity
			MP:0003633	abnormal nervous system physiology
			MP:0003849	greasy coat
			MP:0003879	abnormal hair cell physiology
			MP:0004362	cochlear hair cell degeneration
			MP:0004368	abnormal stria vascularis vasculature morphology
			MP:0004398	cochlear inner hair cell degeneration
			MP:0004404	cochlear outer hair cell degeneration
			MP:0004410	absent endocochlear potential
			MP:0004411	decreased endocochlear potential
			MP:0004740	sensorineural hearing loss
			MP:0004999	abnormal blood-inner ear barrier function
			MP:0005332	abnormal amino acid level
			MP:0005643	decreased dopamine level
			MP:0006325	impaired hearing
			MP:0006332	abnormal cochlear potential
			MP:0006358	absent pinna reflex
			MP:0006403	abnormal cochlear endolymph ionic homeostasis
			MP:0011967	increased or absent threshold for auditory brainstem response
			MP:0011968	decreased threshold for auditory brainstem response
			MP:0013378	increased sebocyte number
KMO	MGI:2138151	kynurenine 3-monooxygenase (kynurenine 3-hydroxylase)	MP:0001415	increased exploration in new environment
			MP:0001764	abnormal homeostasis
			MP:0002573	behavioral despair
			MP:0002797	increased thigmotaxis
			MP:0005584	abnormal enzyme/coenzyme activity
			MP:0013242	abnormal amino acid metabolism
RETSAT	MGI:1914692	retinol saturase (all trans retinol 13,14 reductase)	MP:0000010	abnormal abdominal fat pad morphology
			MP:0005336	abnormal inguinal fat pad morphology
			MP:0005458	increased percent body fat/body weight
			MP:0005561	increased mean corpuscular hemoglobin
			MP:0005564	increased hemoglobin content
			MP:0011167	abnormal adipose tissue development
			MP:0011233	abnormal vitamin A metabolism
GRN	MGI:95832	granulin precursor	MP:0000598	abnormal liver morphology

Symbol	MGI Gene ID	Gene name	MP ID	Term
			MP:0000607	abnormal hepatocyte morphology
			MP:0000837	abnormal hypothalamus morphology
			MP:0001212	skin lesions
			MP:0001259	abnormal body weight
			MP:0001262	decreased body weight
			MP:0001354	increased aggression towards males
			MP:0001360	abnormal social investigation
			MP:0001363	increased anxiety-related response
			MP:0001378	abnormal ejaculation
			MP:0001405	impaired coordination
			MP:0001426	polydipsia
			MP:0001441	increased grooming behavior
			MP:0001442	decreased grooming behavior
			MP:0001463	abnormal spatial learning
			MP:0001473	reduced long term potentiation
			MP:0001752	abnormal hypothalamus secretion
			MP:0001762	polyuria
			MP:0001859	kidney inflammation
			MP:0001900	impaired synaptic plasticity
			MP:0002083	premature death
			MP:0002136	abnormal kidney physiology
			MP:0002152	abnormal brain morphology
			MP:0002175	decreased brain weight
			MP:0002229	neurodegeneration
			MP:0002412	increased susceptibility to bacterial infection
			MP:0002451	abnormal macrophage physiology
			MP:0002705	dilated renal tubules
			MP:0002797	increased thigmotaxis
			MP:0002912	abnormal excitatory postsynaptic potential
			MP:0002981	increased liver weight
			MP:0002988	decreased urine osmolality
			MP:0003068	enlarged kidney
			MP:0003244	loss of dopaminergic neurons
			MP:0003354	astrocytosis
			MP:0003461	abnormal response to novel object
			MP:0003633	abnormal nervous system physiology
			MP:0003691	abnormal microglial cell physiology

Symbol	MGI Gene ID	Gene name	MP ID	Term
			MP:0003862	decreased aggression towards males
			MP:0003917	increased kidney weight
			MP:0004022	abnormal cone electrophysiology
			MP:0004250	tau protein deposits
			MP:0004811	abnormal neuron physiology
			MP:0004860	dilated kidney collecting duct
			MP:0005165	increased susceptibility to injury
			MP:0005418	abnormal circulating hormone level
			MP:0005610	increased circulating antidiuretic hormone level
			MP:0005618	decreased urine potassium level
			MP:0006303	abnormal retinal nerve fiber layer morphology
			MP:0008056	abnormal retinal ganglion cell morphology
			MP:0008067	retinal ganglion cell degeneration
			MP:0008143	abnormal dendrite morphology
			MP:0008415	abnormal neurite morphology
			MP:0008432	abnormal long term spatial reference memory
			MP:0008560	increased tumor necrosis factor secretion
			MP:0008657	increased interleukin-1 beta secretion
			MP:0008660	increased interleukin-10 secretion
			MP:0008663	increased interleukin-12 secretion
			MP:0008705	increased interleukin-6 secretion
			MP:0008722	abnormal chemokine secretion
			MP:0008770	decreased survivor rate
			MP:0008842	lipofuscinosis
			MP:0008845	abnormal paraventricular hypothalamic nucleus morphology
			MP:0008846	abnormal supraoptic nucleus morphology
			MP:0008918	microgliosis
			MP:0008986	abnormal liver parenchyma morphology
			MP:0009454	impaired contextual conditioning behavior
			MP:0009538	abnormal synapse morphology
			MP:0009615	abnormal zinc homeostasis
			MP:0009936	abnormal dendritic spine morphology
			MP:0010080	abnormal hepatocyte physiology
			MP:0010369	abnormal thalamus neuron morphology
			MP:0011436	decreased urine magnesium level
			MP:0011444	abnormal renal water homeostasis
			MP:0011451	increased susceptibility to dopaminergic neuron neurotoxicity

Symbol	MGI Gene ID	Gene name	MP ID	Term
			MP:0011471	decreased urine creatinine level
			MP:0011612	increased circulating ghrelin level
			MP:0011939	increased food intake
			MP:0011941	increased fluid intake
			MP:0011975	neuronal cytoplasmic inclusions
			MP:0012143	decreased a-wave amplitude
			MP:0012144	decreased b-wave amplitude
			MP:0014062	nervous system inclusion bodies
			MP:0020427	increased hepatocyte karyomegaly
			MP:0020508	decreased dendritic spine density

Note: Known phenotypes directly related to heart morphologies and physiologies are marked in red.

Table S10: Parallel genes among lowland mammals with known phenotypes in Mouse Genome Informatics (MGI) database

Symbol	MGI Gene ID	Gene name	MP ID	Term
RHOBTB3	MGI:1920546	Rho-related BTB domain	MP:0000438	abnormal cranium morphology
			MP:0000443	abnormal snout morphology
			MP:0001258	decreased body length
			MP:0001262	decreased body weight
			MP:0001732	postnatal growth retardation
			MP:0001921	reduced fertility
			MP:0002100	abnormal tooth morphology
			MP:0002590	increased mean corpuscular volume
			MP:0002834	decreased heart weight
			MP:0002932	abnormal joint morphology
			MP:0003918	decreased kidney weight
			MP:0003961	decreased lean body mass
			MP:0004852	decreased testis weight
			MP:0004953	decreased spleen weight
			MP:0005353	abnormal patella morphology
			MP:0008770	decreased survivor rate
			MP:0010025	decreased total body fat amount
			MP:0010053	decreased grip strength
			MP:0010124	decreased bone mineral content
			MP:0011110	preweaning lethality, incomplete penetrance
USP8	MGI:1934029	ubiquitin specific peptidase 8	MP:0000267	abnormal heart development
			MP:0000607	abnormal hepatocyte morphology
			MP:0000611	jaundice
			MP:0001654	hepatic necrosis
			MP:0001672	abnormal embryo development
			MP:0001704	abnormal dorsal-ventral axis patterning
			MP:0002083	premature death
			MP:0003326	liver failure
			MP:0003887	increased hepatocyte apoptosis
			MP:0005344	increased circulating bilirubin level
			MP:0011092	embryonic lethality, complete penetrance
			MP:0003984	embryonic growth retardation

Symbol	MGI Gene ID	Gene name	MP ID	Term
JAK2	MGI:96629	Janus kinase 2	MP:0000065	abnormal bone marrow cavity morphology
			MP:0000208	decreased hematocrit
			MP:0000218	increased leukocyte cell number
			MP:0000219	increased neutrophil cell number
			MP:0000220	increased monocyte cell number
			MP:0000221	decreased leukocyte cell number
			MP:0000229	abnormal megakaryocyte differentiation
			MP:0000239	absent common myeloid progenitor cells
			MP:0000240	extramedullary hematopoiesis
			MP:0000245	abnormal erythropoiesis
			MP:0000322	increased granulocyte number
			MP:0000333	decreased bone marrow cell number
			MP:0000601	small liver
			MP:0000628	abnormal mammary gland development
			MP:0000689	abnormal spleen morphology
			MP:0000691	enlarged spleen
			MP:0001545	abnormal hematopoietic system physiology
			MP:0001577	anemia
			MP:0001601	abnormal myelopoiesis
			MP:0001606	impaired hematopoiesis
			MP:0001698	decreased embryo size
			MP:0002083	premature death
			MP:0002123	abnormal definitive hematopoiesis
			MP:0002169	no abnormal phenotype detected
			MP:0002356	abnormal spleen red pulp morphology
			MP:0002357	abnormal spleen white pulp morphology
			MP:0002397	abnormal bone marrow morphology
			MP:0002398	abnormal bone marrow cell morphology/development
			MP:0002417	abnormal megakaryocyte morphology
			MP:0002591	decreased mean corpuscular volume
			MP:0002599	increased mean platelet volume
			MP:0002642	anisocytosis
			MP:0002608	increased hematocrit
			MP:0002447	abnormal erythrocyte morphology

Symbol	MGI Gene ID	Gene name	MP ID	Term
			MP:0002640	reticulocytosis
			MP:0002643	poikilocytosis
			MP:0002813	microcytosis
			MP:0002872	polycythemia
			MP:0002874	decreased hemoglobin content
			MP:0002875	decreased erythrocyte cell number
			MP:0003131	increased erythrocyte cell number
			MP:0003135	increased erythroid progenitor cell number
			MP:0003717	pallor
			MP:0004148	increased compact bone thickness
			MP:0004151	decreased circulating iron level
			MP:0004229	abnormal embryonic erythropoiesis
			MP:0004809	increased hematopoietic stem cell number
			MP:0004810	decreased hematopoietic stem cell number
			MP:0004952	increased spleen weight
			MP:0005013	increased lymphocyte cell number
			MP:0005017	decreased B cell number
			MP:0005097	polychromatophilia
			MP:0005505	thrombocytosis
			MP:0005564	increased hemoglobin content
			MP:0005584	abnormal enzyme/coenzyme activity
			MP:0005621	abnormal cell physiology
			MP:0006269	abnormal mammary gland growth during pregnancy
			MP:0006270	abnormal mammary gland growth during lactation
			MP:0006410	abnormal common myeloid progenitor cell morphology
			MP:0008254	increased megakaryocyte cell number
			MP:0008476	increased spleen red pulp amount
			MP:0008479	decreased spleen white pulp amount
			MP:0009278	abnormal bone marrow cell physiology
			MP:0010178	increased number of Howell-Jolly bodies
			MP:0010249	lactation failure
			MP:0011091	prenatal lethality, complete penetrance
			MP:0010296	increased hemolymphoid system tumor incidence
			MP:0008973	decreased erythroid progenitor cell number

Symbol	MGI Gene ID	Gene name	MP ID	Term
			MP:0010373	myeloid hyperplasia
			MP:0011092	embryonic lethality, complete penetrance
			MP:0011098	embryonic lethality during organogenesis, complete penetrance
			MP:0011099	lethality throughout fetal growth and development, complete penetrance
			MP:0011179	decreased erythroblast number
			MP:0011746	spleen fibrosis
			MP:0011747	myelofibrosis
			MP:0020399	enhanced megakaryocyte emperipolesis
			MP:0030025	giant platelets
MEGF10	MGI:2685177	multiple EGF-like-domains 10	MP:0000849	abnormal cerebellum morphology
			MP:0005240	abnormal amacrine cell morphology
			MP:0006068	abnormal horizontal cell morphology
			MP:0008916	abnormal astrocyte physiology
			MP:0012261	increased hindbrain apoptosis
SERINC1	MGI:1926228	serine incorporator 1	MP:0001258	decreased body length
			MP:0001262	decreased body weight
			MP:0003961	decreased lean body mass
SNAP91	MGI:109132	synaptosomal-associated protein 91	MP:0001262	decreased body weight
			MP:0001364	decreased anxiety-related response
			MP:0001399	hyperactivity
			MP:0001447	abnormal nest building behavior
			MP:0001513	limb grasping
			MP:0001732	postnatal growth retardation
			MP:0002083	premature death
			MP:0002206	abnormal CNS synaptic transmission
			MP:0002945	abnormal inhibitory postsynaptic currents
			MP:0003461	abnormal response to novel object
			MP:0003997	tonic-clonic seizures
			MP:0004753	abnormal miniature excitatory postsynaptic currents
			MP:0004769	abnormal synaptic vesicle morphology
			MP:0004770	abnormal synaptic vesicle recycling
			MP:0004859	abnormal synaptic plasticity
			MP:0002912	abnormal excitatory postsynaptic potential
			MP:0002919	enhanced paired-pulse facilitation

Symbol	MGI Gene ID	Gene name	MP ID	Term
			MP:0004792	abnormal synaptic vesicle number
			MP:0004994	abnormal brain wave pattern
			MP:0011084	lethality at weaning, incomplete penetrance
			MP:0011086	postnatal lethality, incomplete penetrance
			MP:0011270	decreased excitatory postsynaptic current amplitude
			MP:0020357	abnormal excitatory synapse morphology
			MP:0020358	abnormal inhibitory synapse morphology
TNFAIP6	MGI:1195266	tumor necrosis factor alpha induced protein 6	MP:0000242	impaired fertilization
			MP:0001876	decreased inflammatory response
			MP:0001926	female infertility
			MP:0002335	decreased airway responsiveness
			MP:0003355	decreased ovulation rate
			MP:0009374	absent cumulus expansion
TRAIP	MGI:1096377	TRAF-interacting protein	MP:0000352	decreased cell proliferation
			MP:0001698	decreased embryo size
			MP:0002085	abnormal embryonic tissue morphology
			MP:0003984	embryonic growth retardation
			MP:0011097	embryonic lethality between somite formation and embryo turning, complete penetrance
			MP:0011198	absent proamniotic cavity
			MP:0013504	increased embryonic tissue cell apoptosis
UFL1	MGI:1914740	UFM1 specific ligase 1	MP:0000208	decreased hematocrit
			MP:0000221	decreased leukocyte cell number
			MP:0000223	decreased monocyte cell number
			MP:0000334	decreased granulocyte number
			MP:0001262	decreased body weight
			MP:0001263	weight loss
			MP:0001577	anemia
			MP:0001698	decreased embryo size
			MP:0002083	premature death
			MP:0002874	decreased hemoglobin content
			MP:0002875	decreased erythrocyte cell number
			MP:0005016	decreased lymphocyte cell number
			MP:0002942	decreased circulating alanine transaminase level
			MP:0000601	small liver

Symbol	MGI Gene ID	Gene name	MP ID	Term
			MP:0003179	thrombocytopenia
			MP:0005152	pancytopenia
			MP:0005632	decreased circulating aspartate transaminase level
			MP:0008260	abnormal autophagy
			MP:0008973	decreased erythroid progenitor cell number
			MP:0009278	abnormal bone marrow cell physiology
			MP:0009395	increased nucleated erythrocyte cell number
			MP:0010025	decreased total body fat amount
			MP:0011098	embryonic lethality during organogenesis, complete penetrance

Note: Known phenotypes directly related to heart morphologies and physiologies are marked in red.

Table S11: List of 137 placental mammals with RETSAT

Order	Class	Genus	Species	Accession No.
Cingulata	Dasypodidae	Dasypus	*Dasypus novemcinctus*	XP_023443298.1
Eulipotyphla	Erinaceidae	Erinaceus	*Erinaceus europaeus*	XP_016046681.1
Eulipotyphla	Soricidae	Sorex	*Sorex araneus*	XP_004612141.1
Eulipotyphla	Talpidae	Condylura	*Condylura cristata*	XP_004691647.1
Afrotheria	Tenrecidae	Echinops	*Echinops telfairi*	XP_004713929.1
Chiroptera	Pteropodidae	Pteropus	*Pteropus alecto*	XP_015449328.1
Chiroptera	Pteropodidae	Rousettus	*Rousettus aegyptiacus*	XP_015992312.2
Chiroptera	Phyllostomidae	Desmodus	*Desmodus rotundus*	XP_024414216.1
Chiroptera	Vespertilionidae	Eptesicus	*Eptesicus fuscus*	XP_008154129.1
Chiroptera	Vespertilionidae	Myotis	*Myotis lucifugus*	XP_006099957.1
Chiroptera	Vespertilionidae	Myotis	*Myotis brandtii*	XP_005882472.1
Chiroptera	Vespertilionidae	Myotis	*Myotis davidii*	XP_006764069.1
Chiroptera	Vespertilionidae	Miniopterus	*Miniopterus natalensis*	XP_016057274.1
Chiroptera	Rhinolophidae	Rhinolophus	*Rhinolophus sinicus*	XP_019570092.1
Primates	Cebidae	Callithrix	*Callithrix jacchus*	XP_035127993.1
Primates	Cebidae	Saimiri	*Saimiri boliviensis boliviensis*	XP_010328294.1
Primates	Cebidae	Cebus	*Cebus capucinus imitator*	XP_017373447.1
Primates	Cercopithecidae	Cercocebus	*Cercocebus atys*	XP_011919534.1
Primates	Cercopithecidae	Macaca	*Macaca fascicularis*	XP_005575500.1
Primates	Cercopithecidae	Macaca	*Macaca mulatta*	NP_001244492.1
Primates	Cercopithecidae	Macaca	*Macaca nemestrina*	XP_011712099.1
Primates	Cercopithecidae	Papio	*Papio anubis*	XP_003908948.1
Primates	Cercopithecidae	Mandrillus	*Mandrillus leucophaeus*	XP_011821176.1
Primates	Cercopithecidae	Chlorocebus	*Chlorocebus sabaeus*	XP_037863609.1
Primates	Cercopithecidae	Rhinopithecus	*Rhinopithecus bieti*	XP_017714499.1
Primates	Cercopithecidae	Colobus	*Colobus angolensis palliatus*	XP_011819325.1
Primates	Hominidae	Gorilla	*Gorilla gorilla gorilla*	XP_004029584.1
Primates	Hominidae	Pan	*Pan paniscus*	XP_003816634.1
Primates	Hominidae	Pan	*Pan troglodytes*	XP_525801.2
Primates	Hominidae	Pongo	*Pongo abelii*	XP_009235408.2
Primates	Hominidae	Homo	*Homo sapiens*	NP_060220.3
Primates	Cheirogaleidae	Microcebus	*Microcebus murinus*	XP_012629718.1
Primates	Galagidae	Otolemur	*Otolemur garnettii*	XP_003799263.1
Primates	Hylobatidae	Nomascus	*Nomascus leucogenys*	XP_030683856.1
Primates	Indriidae	Propithecus	*Propithecus coquereli*	XP_012499687.1
Carnivora	Canidae	Canis	*Canis lupus familiaris*	XP_540198.1
Carnivora	Canidae	Vulpes	*Vulpes vulpes*	XP_025850218.1
Carnivora	Ursidae	Ailuropoda	*Ailuropoda melanoleuca*	XP_002922894.1
Carnivora	Ursidae	Ursus	*Ursus maritimus*	XP_008698285.1
Carnivora	Mustelidae	Mustela	*Mustela putorius furo*	XP_004742373.1
Carnivora	Felidae	Felis	*Felis catus*	XP_003984273.1
Carnivora	Felidae	Panthera	*Panthera pardus*	XP_019298947.1
Carnivora	Felidae	Panthera	*Panthera tigris altaica*	XP_007082335.1
Carnivora	Felidae	Puma	*Puma concolor*	XP_025788027.1
Carnivora	Felidae	Acinonyx	*Acinonyx jubatus*	XP_026927871.1
Carnivora	Odobenidae	Odobenus	*Odobenus rosmarus divergens*	XP_004415479.1
Carnivora	Phocidae	Neomonachus	*Neomonachus schauinslandi*	XP_021553266.1
Carnivora	Otariidae	Callorhinus	*Callorhinus ursinus*	XP_025724084.1

Artiodactyla	Delphinidae	Orcinus	*Orcinus orca*	XP_004271663.1
Artiodactyla	Monodontidae	Delphinapterus	*Delphinapterus leucas*	XP_022411750.1
Artiodactyla	Physeteridae	Physeter	*Physeter catodon*	XP_007121629.1
Artiodactyla	Suidae	Sus	*Sus scrofa*	XP_003124992.1
Artiodactyla	Hippopotamidae	Hippopotamus	*Hippopotamus amphibius*	Ruminant Genome Project*
Artiodactyla	Camelidae	Camelus	*Camelus bactrianus*	XP_010957426.1
Artiodactyla	Camelidae	Camelus	*Camelus dromedarius*	XP_010996126.1
Artiodactyla	Camelidae	Camelus	*Camelus ferus*	XP_006183675.1
Artiodactyla	Camelidae	Vicugna	*Vicugna pacos*	XP_006203851.1
Artiodactyla	Tragulidae	Tragulus	*Tragulus javanicus*	Ruminant Genome Project*
Artiodactyla	Cervidae	Rangifer	*Rangifer tarandus*	Ruminant Genome Project*
Artiodactyla	Cervidae	Odocoileus	*Odocoileus virginianus texanus*	XP_020745081.1
Artiodactyla	Cervidae	Muntiacus	*Muntiacus reevesi*	KAB0381457.1
Artiodactyla	Cervidae	Muntiacus	*Muntiacus muntjak*	KAB0359388.1
Artiodactyla	Cervidae	Muntiacus	*Muntiacus crinifrons*	Ruminant Genome Project*
Artiodactyla	Cervidae	Przewalskium	*Przewalskium albirostris*	Ruminant Genome Project*
Artiodactyla	Antilocapridae	Antilocapra	*Antilocapra americana*	Ruminant Genome Project*
Artiodactyla	Giraffidae	Giraffa	*Giraffa camelopardalis*	Ruminant Genome Project*
Artiodactyla	Giraffidae	Okapia	*Okapia johnstoni*	Ruminant Genome Project*
Artiodactyla	Bovidae	Aepyceros	*Aepyceros melampus*	Ruminant Genome Project*
Artiodactyla	Bovidae	Ammotragus	*Ammotragus lervia*	Ruminant Genome Project*
Artiodactyla	Bovidae	Bos	*Bos taurus*	NP_001095749.2
Artiodactyla	Bovidae	Bos	*Bos indicus*	XP_027411356.1
Artiodactyla	Bovidae	Bos	*Bos mutus*	XP_005891742.1
Artiodactyla	Bovidae	Capra	*Capra hircus*	XP_005686784.1
Artiodactyla	Bovidae	Connochaetes	*Connochaetes taurinus*	Ruminant Genome Project*
Artiodactyla	Bovidae	Damaliscus	*Damaliscus lunatus*	Ruminant Genome Project*
Artiodactyla	Bovidae	Ovis	*Ovis aries musimon*	XP_004005915.2
Artiodactyla	Bovidae	Ovis	*Ovis ammon*	Ruminant Genome Project*
Artiodactyla	Bovidae	Tragelaphus	*Tragelaphus oryx*	Ruminant Genome Project*
Artiodactyla	Bovidae	Tragelaphus	*Tragelaphus strepsiceros*	Ruminant Genome Project*
Artiodactyla	Bovidae	Tragelaphus	*Tragelaphus buxtoni*	Ruminant Genome Project*
Artiodactyla	Bovidae	Tragelaphus	*Tragelaphus eurycerus*	Ruminant Genome Project*
Artiodactyla	Bovidae	Tragelaphus	*Tragelaphus spekii*	Ruminant Genome Project*
Artiodactyla	Bovidae	Oryx	*Oryx gazella*	Ruminant Genome Project*
Artiodactyla	Bovidae	Syncerus	*Syncerus caffer*	Ruminant Genome Project*
Artiodactyla	Bovidae	Nanger	*Nanger granti*	Ruminant Genome Project*
Artiodactyla	Bovidae	Bison	*Bison bison bison*	XP_010860484.1
Artiodactyla	Bovidae	Antidorcas	*Antidorcas marsupialis*	Ruminant Genome Project*
Artiodactyla	Bovidae	Pantholops	*Pantholops hodgsonii*	XP_005970951.1
Artiodactyla	Bovidae	Pseudois	*Pseudois nayaur*	Ruminant Genome Project*
Artiodactyla	Bovidae	Neotragus	*Neotragus moschatus*	Ruminant Genome Project*
Artiodactyla	Bovidae	Eudorcas	*Eudorcas thomsonii*	Ruminant Genome Project*
Artiodactyla	Bovidae	Litocranius	*Litocranius walleri*	Ruminant Genome Project*
Artiodactyla	Bovidae	Bubalus	*Bubalus bubalis*	XP_006061146.1
Artiodactyla	Bovidae	Sylvicapra	*Sylvicapra grimmia*	Ruminant Genome Project*

Artiodactyla	Bovidae	Cephalophus	*Cephalophus harveyi*	Ruminant Genome Project*
Artiodactyla	Bovidae	Procapra	*Procapra przewalskii*	Ruminant Genome Project*
Artiodactyla	Moschidae	Moschus	*Moschus berezovskii*	Ruminant Genome Project*
Artiodactyla	Lipotidae	Lipotes	*Lipotes vexillifer*	XP_007470658.1
Artiodactyla	Phocoenidae	Neophocaena	*Neophocaena asiaeorientalis*	XP_024599653.1
Artiodactyla	Balaenopteridae	Balaenoptera	*Balaenoptera acutorostrata scammoni*	XP_007175426.1
Proboscidea	Elephantidae	Loxodonta	*Loxodonta africana*	XP_003420461.1
Perissodactyla	Equidae	Equus	*Equus asinus*	XP_014708318.1
Perissodactyla	Equidae	Equus	*Equus caballus*	XP_001497500.2
Perissodactyla	Equidae	Equus	*Equus przewalskii*	XP_008514183.1
Perissodactyla	Rhinocerotidae	Ceratotherium	*Ceratotherium simum simum*	XP_004437263.1
Pholidota	Manidae	Manis	*Manis javanica*	XP_017529752.1
Lagomorpha	Ochotonidae	Ochotona	*Ochotona princeps*	XP_004590854.1
Lagomorpha	Ochotonidae	Ochotona	*Ochotona curzoniae*	Ruminant Genome Project*
Lagomorpha	Leporidae	Oryctolagus	*Oryctolagus cuniculus*	XP_002709724.1
Rodentia	Sciuridae	Marmota	*Marmota marmota marmota*	XP_015361794.1
Rodentia	Sciuridae	Urocitellus	*Urocitellus parryii*	XP_026269886.1
Rodentia	Sciuridae	Ictidomys	*Ictidomys tridecemlineatus*	XP_005338514.1
Rodentia	Sciuridae	Sciurus	*Sciurus vulgaris*	Ruminant Genome Project*
Rodentia	Sciuridae	Spermophilus	*Spermophilus dauricus*	Ruminant Genome Project*
Rodentia	Heteromyidae	Dipodomys	*Dipodomys ordii*	XP_012890906.1
Rodentia	Cricetidae	Cricetulus	*Cricetulus griseus*	XP_027285265.1
Rodentia	Cricetidae	Mesocricetus	*Mesocricetus auratus*	XP_005078329.1
Rodentia	Cricetidae	Microtus	*Microtus ochrogaster*	XP_026643771.1
Rodentia	Cricetidae	Peromyscus	*Peromyscus maniculatus bairdii*	XP_006996070.1
Rodentia	Muridae	Mus	*Mus caroli*	XP_021021251.1
Rodentia	Muridae	Mus	*Mus musculus*	NP_080435.3
Rodentia	Muridae	Mus	*Mus pahari*	XP_021046668.1
Rodentia	Muridae	Rattus	*Rattus norvegicus*	NP_659552.1
Rodentia	Caviidae	Cavia	*Cavia porcellus*	XP_003468949.1
Rodentia	Caviidae	Cavia	*Cavia aperea*	Ruminant Genome Project*
Rodentia	Octodontidae	Octodon	*Octodon degus*	XP_004642866.1
Rodentia	Bathyergidae	Heterocephalus	*Heterocephalus glaber*	XP_004844681.1
Rodentia	Bathyergidae	Fukomys	*Fukomys damarensis*	XP_010633552.1
Rodentia	Chinchillidae	Chinchilla	*Chinchilla lanigera*	XP_005385493.1
Rodentia	Dipodidae	Jaculus	*Jaculus jaculus*	XP_004660588.1
Rodentia	Castoridae	Castor	*Castor canadensis*	XP_020018949.1
Rodentia	Spalacidae	Eospalax	*Eospalax fontanierii baileyi*	Ruminant Genome Project*
Rodentia	Spalacidae	Nannospalax	*Nannospalax galili*	XP_008838476.1
Macroscelidea	Macroscelididae	Elephantulus	*Elephantulus edwardii*	XP_006900457.1
Sirenia	Trichechidae	Trichechus	*Trichechus manatus latirostris*	XP_012414510.1
Afrotheria	Chrysochloridae	Chrysochloris	*Chrysochloris asiatica*	XP_006866653.1
Scandentia	Tupaiidae	Tupaia	*Tupaia chinensis*	XP_006149194.1

*http://animal.nwsuaf.edu.cn/code/index.php/RGD

Table S12: Examination of selection for the parallel substitution in RETSAT among 137 placental mammals

Observed number of parallel substitutions	Expected number of parallel substitutions		*P* value[1]
	Neutral substitution model	Number of substitutions	
1	JTT-f_{gene}	0	0
1	JTT-f_{site}	6.00E-07	6.00E-07

Note: [1]The expected parallel evolution sites was calculation followed the method developed by Zou and Zhang (2015).
*, *P* value < 0.05; **, P value <0.01; ***, P value <0.001.